Wu et al. *Zool. Res.* 2022, 43(3): 457−468
https://doi.org/10.24272/j.issn.2095-8137.2021.469

ZR | Zoological Research

Article Open Access

Combinational benefit of antihistamines and remdesivir for reducing SARS-CoV-2 replication and alleviating inflammation-induced lung injury in mice

Meng-Li Wu[1,2,#], Feng-Liang Liu[3,#], Jing Sun[4,#], Xin Li[2], Jian-Ru Qin[1], Qi-Hong Yan[4], Xia Jin[1], Xin-Wen Chen[2], Yong-Tang Zheng[3,*], Jin-Cun Zhao[4,*], Jian-Hua Wang[2,4,5,*]

[1] *College of Life Science*, *Henan Normal University*, *Xinxiang*, *Henan* 453007, *China*

[2] *Guangzhou Institutes of Biomedicine and Health*, *Chinese Academy of Sciences*, *Guangzhou*, *Guangdong* 510530, *China*

[3] *Key Laboratory of Animal Models and Human Disease Mechanisms of the Chinese Academy of Sciences*, *Kunming Institute of Zoology*, *Chinese Academy of Sciences*, *Kunming*, *Yunnan* 650223, *China*

[4] *State Key Laboratory of Respiratory Disease*, *National Clinical Research Center for Respiratory Disease*, *Guangzhou Institute of Respiratory Health*, *First Affiliated Hospital of Guangzhou Medical University*, *Guangzhou*, *Guangdong* 510182, *China*

[5] *University of Chinese Academy of Sciences*, *Beijing* 100049, *China*

ABSTRACT

COVID-19 is an immune-mediated inflammatory disease caused by SARS-CoV-2 infection, the combination of anti-inflammatory and antiviral therapy is predicted to provide clinical benefits. We recently demonstrated that mast cells (MCs) are an essential mediator of SARS-CoV-2-initiated hyperinflammation. We also showed that spike protein-induced MC degranulation initiates alveolar epithelial inflammation for barrier disruption and suggested an off-label use of antihistamines as MC stabilizers to block degranulation and consequently suppress inflammation and prevent lung injury. In this study, we emphasized the essential role of MCs in SARS-CoV-2-induced lung lesions *in vivo*, and demonstrated the benefits of co-administration of antihistamines and antiviral drug remdesivir in SARS-CoV-2-infected mice. Specifically, SARS-CoV-2 spike protein-induced MC degranulation resulted in alveolar-capillary injury, while pretreatment of pulmonary microvascular endothelial cells with antihistamines prevented adhesion junction disruption; predictably, the combination of antiviral drug remdesivir with the antihistamine loratadine, a histamine receptor 1 (HR1) antagonist, dampened viral replication and inflammation, thereby greatly reducing lung injury. Our findings emphasize the crucial role of MCs in SARS-CoV-2-induced inflammation and lung injury and provide a feasible combination antiviral and anti-inflammatory therapy for COVID-19 treatment.

Keywords: SARS-CoV-2; Mast cell; Remdesivir;

Received: 18 March 2022; Accepted: 19 April 2022; Online: 25 April 2022

Foundation items: This work was supported by the National Natural Science Foundation of China (82172242, 81873965), State Key Laboratory of Respiratory Disease, Guangzhou, China (SKLRD-OP-202207), National Key R&D Program of China (2020YFC0842000), Natural Science Foundation of Guangdong (2022A1515012053), and Key Project from the Chinese Academy of Sciences (QYZDB-SSW-SMC059)

[#]Authors contributed equally to this work

*Corresponding authors, E-mail: zhengyt@mail.kiz.ac.cn; zhaojincun@gird.cn; wang_jianhua@gibh.ac.cn

Antihistamine; Combinational therapy

INTRODUCTION

Coronavirus disease 2019 (COVID-19) is caused by severe acute respiratory syndrome coronavirus 2 (SARS-CoV-2) infection. This infection dysregulates the immune system by inducing hyperinflammatory responses, which produce excessive pro-inflammatory mediators that trigger acute lung injury, septic shock, acute respiratory distress syndrome, and multiple organ failure, thus contributing to significant morbidity and mortality (Attiq et al., 2021; Chen et al., 2020; Huang et al., 2021; Qin et al., 2020; Song et al., 2020; Tian et al., 2021; Wang et al., 2020a; Xu et al., 2020). To curtail this disease, the US Food and Drug Administration (FDA) has approved and authorized two mRNA-based vaccines (Pfizer-BioNTech, Moderna) and one recombinant adenovirus-26 vaccine (Janssen, Ad26.COV2.S) for population use, while the World Health Organization (WHO) has approved the BBIBP-CorV and CoronaVac inactivated vaccines, both of which were developed in China. Globally more than 100 candidate vaccines, including 20 inactivated SARS-CoV-2 vaccines, are under development (Marfe et al, 2021).

Considering the limited durability of protection conferred by existing vaccines and the real-life reduction in vaccine effectiveness due to the emergence of SARS-CoV-2 variants, efficacious pharmacological treatment for COVID-19 is still urgently needed. Several drugs repurposed from viral disease treatments have been tested against COVID-19, including remdesivir, favipiravir, and lopinavir/ritonavir, which interfere with the function of SARS-CoV-2 RNA-dependent RNA-polymerases (RdRp) (Biswas et al, 2021). The ribonucleoside analogue molnupiravir (EIDD-2801, MK-4482), developed by Merck and Ridgeback, has been approved in the UK for the oral treatment of COVID-19 (Mahase, 2021a;c). Paxlovid (PF-07311332 and ritonavir), another oral-administration candidate developed by Pfizer, is reported to reduce the risk of hospitalization or death by 89% compared to placebo in non-hospitalized high-risk adults with COVID-19 (Mahase, 2021b). Furthermore, the Janus kinase (JAK) 1/2 inhibitor baricitinib has been approved for use in Japan (23 April 2021) (Mouffak et al, 2021) and several monoclonal antibodies (mAbs) are under development for COVID-19 treatment and/or prophylaxis (Mouffak et al, 2021).

Remdesivir is a nucleotide analogue that can efficiently inhibit viral RdRp, with well-established activity against various flaviviruses (Konkolova et al, 2020). Remdesivir shows efficient repression of SARS-CoV-2 replication in cellular and mouse models (Pruijssers et al, 2020), and shortens recovery time in adult patients following early administration (Beigel et al, 2020; De Clercq, 2021; Rochwerg et al, 2020; Wang et al, 2020b, 2020c). Thus, remdesivir (Veklury) has been approved by the US FDA for the treatment of COVID-19 in adults and children older than 12 years (Rubin et al, 2020).

Many COVID-19 patients manifest symptoms associated with inflammation (Attiq et al, 2021; Daher, 2021), and the combination of anti-inflammatory and antiviral therapy seems to be beneficial (De Clercq, 2021; Mouffak et al, 2021). The combination of remdesivir with corticosteroids (dexamethasone) reduces both viral load and inflammation in hamster models of SARS-CoV-2 infection (Ye et al, 2021), and reduces the 30-day mortality rate from 19.7% to 12.6% in severe COVID-19 patients (Benfield et al, 2021). Remdesivir combined with the JAK 1/2 inhibitor baricitinib is superior to remdesivir alone in shortening recovery time and accelerating clinical improvement, especially in patients receiving high-flow oxygen or noninvasive ventilation, with fewer serious adverse events (Kalil et al, 2021).

Mast cells (MCs) are tissue-resident cells strategically placed throughout the host-environment interface. In addition to being the main effector cells in allergic response, MCs also play regulatory roles in various pathophysiological processes (Komi et al., 2020; Lam et al., 2021). Postmortem lung biopsies of COVID-19 patients show a massive increase in the density of perivascular and septal MCs (Da Silva Motta Junior et al., 2020; Dos Santos Miggiolaro et al., 2020). SARS-CoV-2 infection is reported to trigger MC infiltration into the pulmonary parenchyma of African green monkeys (Malone et al, 2021). We also recently demonstrated that SARS-CoV-2 triggers rapid degranulation of MCs and initiates alveolar epithelial inflammation and subsequent lung injury in mice (Wu et al, 2021). These studies suggest that MCs may play a critical role in the pathogenesis of SARS-CoV-2 and may be a novel therapeutic cell target for the treatment of COVID-19 (Lam et al, 2021; Malone et al, 2021; Murdaca et al, 2021). Indeed, we previously found that administration of clinically approved MC stabilizers (i.e., antihistamines ebastine and loratadine) dampens SARS-CoV-2-induced production of pro-inflammatory factors and prevents lung injury in mice (Wu et al, 2021). In this study, we revealed the essential role of MCs in SARS-CoV-2-induced lung injury. Notably, we investigated the potential benefits of suppressing viral replication and alleviating hyperinflammation by co-administration of antihistamines and remdesivir in a mouse model of SARS-CoV-2 infection.

MATERIALS AND METHODS

Ethics statement

All animal experiments were approved by the Institutional Animal Care and Use Committee of the Guangzhou Institutes of Biomedicine, Chinese Academy of Sciences (Approval No. N2021016). All SARS-CoV-2 animal model experiments and protocols were discussed extensively with biosafety officers and facility managers. All animal and viral experiments were conducted within an animal biosafety level 3 (ABSL-3) facility.

Cells

Human MCs (LAD2) were cultured in RPMI 1640 medium (Gibco, USA) containing 10% fetal bovine serum (FBS) (Gibco, USA) with 100 U/mL penicillin and 100 μg/mL streptomycin. For degranulation, the LAD2 cells were grown in StemPro-34 medium (Gibco, USA) supplemented with 100 μg/mL stem cell factor (Novoprotein, China), 10 μg/mL interleukin-6 (IL-6) (Novoprotein, China), nutrient supplement (NS) (Gibco, USA), 100 U/mL penicillin (Invitrogen, USA), 100 μg/mL of streptomycin (Invitrogen, USA), and 2 mmol/L L-glutamine (Gibco, USA). Human lung microvascular

endothelial cells (HULEC-5a) were cultured in MCDB131 medium (Gibco, USA) containing 10 ng/mL epidermal growth factor (EGF) (R&D, USA), 1 μg/mL hydrocortisone (Apexbio, China), 10 mmol/L L-glutamine (Gibco, USA), 10% FBS (Gibco, USA), 100 U/mL penicillin, and 100 μg/mL streptomycin.

Mast cell degranulation

The LAD2 cells (3×10^5) were exposed to recombinant receptor-binding domain (RBD) derived from wild-type SARS-CoV-2 (GenScript, Z03483, China) or the 501Y.V2 variant (GenScript, Z03531, China) for indicated times. The cells were fixed with 4% paraformaldehyde (Sigma-Aldrich, USA) at room temperature (RT) for 30 min, then washed three times with phosphate-buffered saline (PBS), and incubated with anti-avidin-FITC (500 ng/mL, Invitrogen, A821, USA) diluted in permeabilized buffer (1% FBS and 0.2% Triton X-100 in PBS) for 1 h at 4 °C. After washing, cells were detected with flow cytometry (BD Accuri C6, USA) and analyzed with FlowJo v7.6.1 (USA). Histamine in the LAD2 cell culture supernatants was quantified with an enzyme-linked immunosorbent assay (ELISA) kit according to the manufacturer's instructions (Sangon Biotech, D751012, China). Compound 48/80 (C48/80) (4 μg/mL) (Sigma, C2313, USA), which can stimulate MC degranulation, was used as the control. All experiments were performed at the Guangzhou Institutes of Biomedicine and Health, Chinese Academy of Sciences.

Mouse infection

Specific pathogen-free 6-week-old female wild-type BALB/c mice were infected intranasally with the 501Y.V2 SARS-CoV-2 variant (B.1.351, GISAID: EPI_ISL_2423556) at a 50% cell culture infective dose (CCID50) of 7.1×10^4. The 501Y.V2 strain was provided by Guangzhou Medical University, Guangdong, China. Loratadine (Lor.) (10 mg/kg) (Sigma-Aldrich, USA) was administered intraperitoneally (i.p.) 1 day before infection and Lor. treatment was continued each day over the course of infection; remdesivir (25 mg/kg) was administered (i.p.) at the time of infection and used once daily until euthanasia. Five mice in each group and three mice in control group. The lungs were collected at 3 days post-infection (dpi) for pathological, virological, and immunological analyses. Experiments were performed in the ABSL-3 facility at the First Affiliated Hospital of Guangzhou Medical University.

Pathology

The lungs of mice were harvested and fixed in zinc formalin. For routine histology, tissue sections (~4 μm each) were stained with hematoxylin and eosin (H&E) or toluidine blue. In brief, the tissue sections were stained with 1% toluidine blue (Sigma-Aldrich, USA) for 1 h at RT, then washed in distilled water three times, anhydrous ethanol two times, and covered with a coverslip. Pathological score was assessed according to the degree of lung tissue lesions, including alveolar septal thickening, hemorrhage, inflammatory cell infiltration, and consolidation. Semi-quantitative assessment was determined as follows: 0: No alveolar septal thickening; 1: Very mild alveolar septal thickening, with area of alveolar septal thickening, hemorrhage, and inflammatory cell infiltration <10%; 2: Mild alveolar septal thickening, with area of alveolar septal thickening, hemorrhage, and inflammatory cell infiltration 10%–25%; 3: Moderate alveolar septal thickening, with area of alveolar septal thickening, hemorrhage, inflammatory cell infiltration, mucosa desquamation, and fibrinous exudate 25%–50%; 4: Marked alveolar septal thickening, with area of alveolar septal thickening, hemorrhage, inflammatory cell infiltration, mucosa desquamation, and fibrinous exudate 50%–75%; 5: Very marked alveolar septal thickening, with area of alveolar septal thickening, hemorrhage, inflammatory cell infiltration, mucosa desquamation, and fibrinous exudate >75%.

For immunofluorescence, frozen lung sections were blocked with 5% bovine serum albumin (BSA) in PBS at RT for 1 h, incubated with anti-VE-cadherin primary antibodies (Abcam, ab205336, UK) for 2 h at RT, then incubated with Alexa Flour 488-labeled goat anti-rabbit IgG (Invitrogen, A11034, USA) for 1 h at RT. The sections were further incubated with DAPI (Beyotime, China) and analyzed using a Pannoramic MIDI slice scanning apparatus (3DHISTECH, USA). The fixed tissue sections were stained at the Pathology Center of the Guangzhou Institutes of Biomedicine and Health, Chinese Academy of Sciences.

Flow cytometry and fluorescence microscopy

To detect VE-cadherin expression using flow cytometry, HULEC-5a cells (1×10^5) were treated with RBD proteins (2 μg/mL) derived from wild-type SARS-CoV-2 (GenScript, Z03483, China) and co-cultured with LAD2 cells (1×10^5) in the presence or absence of RBD proteins (2 μg/mL) or stimulated with RBD-treated LAD2 cell culture supernatants (300 μL) for 48 h at 37 °C. Medium treatment was used as the control. In other groups (3 repeats), Lor. (2.5 μg/mL, Selleck , China), ebastine (Eba., 1.5 μg/mL, Selleck, China), or ketotifen fumarate (Ket., 4 μg/mL, Yuanye Biology, S46226, China) was used to pretreat HULEC-5a cells for 2 h before stimulation. The cells were harvested and blocked with 5% BSA for 1 h at RT, incubated with anti-VE-cadherin antibodies (Cell Signaling Technology, D87F2, USA) for 2 h at RT, washed with FACS buffer, incubated with Alexa Flour 488-labeled goat anti-rabbit (Invitrogen, A11034, USA) for 30 min at RT, then analyzed using flow cytometry. The HULEC-5a cells were also seeded on a coverslip to form a monolayer to observe VE-cadherin fluorescence using an Olympus CKX53 fluorescence microscope (Japan).

To detect IL-6 expression at the protein level, HULEC-5a cells (3×10^5) were treated with LAD2 culture supernatant (250 μL) for 24 h at 37 °C, then harvested, mixed with a leukocyte activation cocktail containing BD GolgiPlug (BD, 550583, USA), and cultured for 6 h at 37 °C. Following activation, cells were washed with FACS buffer. The BD Cytofix/Cytoperm solution (BD, 554722, USA) was used for the simultaneous fixation and permeabilization of cells for 20 min at 4 °C before intracellular cytokine staining. Rat anti-human IL-6-PE (BD, MQ2-6A3, USA) was added, and the cells were further incubated at 4 °C overnight. After washing, the cells were resuspended in FACS buffer, then analyzed using flow cytometry (BD Accuri C6, USA) and FlowJo v7.6.1 (USA). In other groups (3 repeats), Lor. (2.5 μg/mL, Selleck,

China), Eba.(1.5 μg/mL, Selleck, China), or Ket. (4 μg/mL, Yuanye Biology, S46226, China) was used to pretreat HULEC-5a cells for 2 h at 37 °C before stimulation with the LAD2 culture supernatant. All experiments were performed at the Guangzhou Institutes of Biomedicine and Health, Chinese Academy of Sciences.

Real-time polymerase chain reaction (RT-PCR)

Total RNA from cells/tissues was extracted using TRIzol Reagent (Invitrogen, USA), then reverse transcribed into cDNA using a synthesis kit (TOYOBO, FSQ-301, Japan) according to the manufacturer's instructions. RT-PCR was carried out using SYBR qPCR Mix (GeneSTAR, A33-101, China) with the following thermal cycling conditions: initial denaturation at 95 °C for 2 min, amplification with 40 cycles of denaturation at 95 °C for 15 s, primer annealing at 60 °C for 15 s, and extension at 72 °C for 30 s. The data were analyzed by SYBR green-based semi-quantification and normalized with *GAPDH*. RT-PCR was performed on the Bio-Rad CFX96 Real-Time PCR system (USA). Mouse-extracted RNA was used to measure copies of the SARS-CoV-2 nucleocapsid gene using a THUNDERBIRD Probe One-step qRT-PCR Kit (TOYOBO, Japan). The standard samples were provided by Dr. Ling Chen (Guangzhou Institutes of Biomedicine and Health, Chinese Academy of Sciences, China). The primers and probes used for RT-PCR are listed in Supplementary Table S1. Mouse tissue RNA was isolated in the ABSL-3 facility at the First Affiliated Hospital of Guangzhou Medical University, and RT-PCR was performed at the Guangzhou Institutes of Biomedicine and Health, Chinese Academy of Sciences.

RNA sequencing (RNA-seq) and data analysis

The HULEC-5a cells were cultured with RBD-treated LAD2 cell culture supernatants for 24 h at 37 °C. Total RNA was extracted using TRIzol (Invitrogen , USA) according to the manufacturer's protocols, and ribosomal RNA was removed using a QIAseq FastSelect-rRNA HMR Kit (Qiagen, Germany). Fragmented RNA (average length ~200 bp) was subjected to first- and second-strand cDNA synthesis, followed by adaptor ligation and enrichment under a low cycle according to the instructions provided with the NEBNext Ultra RNA Library Prep Kit for Illumina (New England Biolabs, USA). The purified library products were evaluated using Agilent 2200 TapeStation and Qubit v2.0 (Life Technologies, USA). The libraries were paired-end sequenced (PE150, sequencing reads 150 bp) at Genewiz (China) using the Illumina HiSeq 3000 platform.

Raw RNA-seq reads were filtered using Trimmomatic v0.36. The filtered reads were mapped to the human (hg38) reference genome using HISAT v2.1 and corresponding gene annotations (GRCh38.p13) with default settings. Total counts per mapped gene were determined using the FeatureCounts function in the SubReads package v1.5.3 with default parameters. The counts matrix was then obtained using the feature counts as input for differential gene expression analysis with the Bioconductor package DESeq2 v1.26 in R v4.0. Gene counts with more than five reads in a single sample or more than 50 total reads across all samples were retained for further analysis. The filtered counts matrix was normalized using the DESeq2 method to remove library-specific artifacts. Principal component analysis was based on global transcriptome data using the build-in function prcomp in R. Genes with a log2 fold-change>1 or <–1 and adjusted P<0.05 (Benjamini-Hochberg corrected) were considered significant. Transcription factor and functional enrichment analyses were performed using Metascape (Zhou et al, 2019) (https://metascape.org/gp/index.html#/main/step1). Gene set enrichment analysis (GSEA) was conducted using the R package clusterProfiler v3.18.1.

Statistical analysis

GraphPad Prism v8.0 was used for statistical analysis. For direct intragroup comparison, student's unpaired two-tailed *t*-test was performed to analyze significant differences. For comparisons among multiple groups, one-way analysis of variance (ANOVA) was performed. Significance levels were determined at *: P<0.05; **: P<0.01; ***: P<0.001.

RESULTS

Spike-induced MC degranulation predisposes microvascular endothelial cells to damage

We previously demonstrated that SARS-CoV-2 spike/RBD protein-induced MC degranulation initiates alveolar epithelial inflammation and barrier disruption in mice (Wu et al, 2021). To investigate whether the presence of MCs or their degranulation induces alveolar-capillary injury, HULEC-5a cells were seeded on a coverslip to form a cell monolayer, then treated with spike/RBD-stimulated LAD2 cell culture supernatant (Deg. Supern.) for 48 h. The adherent junction protein VE-cadherin in the HULEC-5a cells was examined as an indicator of microvascular endothelial barrier integrity (Wang et al, 2020a). Results showed that Deg. Supern. markedly altered VE-cadherin organization in the HULEC-5a cells (Figure 1A). Direct stimulation with spike/RBD for 48 h or co-culture with LAD2 cells did not disrupt VE-cadherin; however, the addition of spike/RBD to the co-culture of LAD2/HULEC-5a cells (LAD2/RBD) altered VE-cadherin organization (Figure 1B).

Histamine receptor 1 (HR1) antagonists (i.e., Ket., Eba., and Lor.) are routinely used to treat allergies in humans (Slater et al, 1999). In addition to their primary mechanism of antagonizing histamine at HR1, they may also act on other mediators of allergic reactions (Abdelaziz et al, 2000; Slater et al, 1999). Thus, we next investigated whether these antihistamines could provide protection against MC degranulation-induced disruption of adhesion junctions. HULEC-5a cell monolayers were first pretreated with the antihistamines, then co-cultured with LAD2 cells in the presence of the spike/RBD protein or directly treated with the spike/RBD-stimulated LAD2 cell culture supernatant. Results showed that pretreatment with the antihistamines rescued MC degranulation-triggered disruption of VE-cadherin (Figure 1C).

The MC degranulation-induced disruption of VE-cadherin in the HULEC-5a cells was quantified using flow cytometry. Results showed that treatment with the spike/RBD-stimulated LAD2 cell culture supernatant (Deg. Supern.) (Figure 1D) or

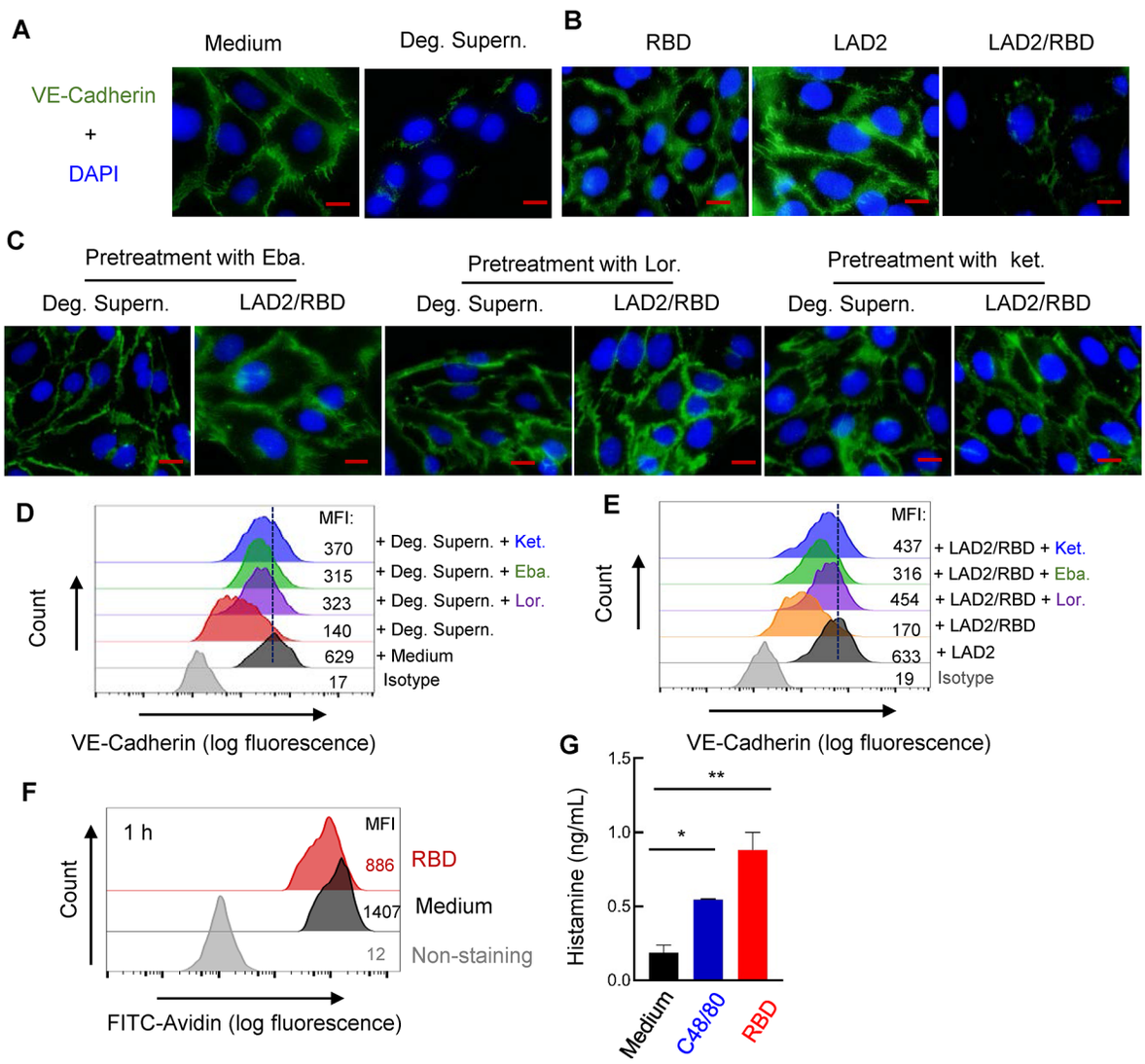

Figure 1 MC degranulation disrupts VE-cadherin in HULEC-5a cells

A–C: VE-cadherin expression observed by fluorescence microscopy. HULEC-5a cells (1×10^5) were seeded on a coverslip to form a monolayer, then treated with RBD-stimulated LAD2 cell culture supernatant (Deg. Supern.) (300 μL), or Medium (*A*) with RBD protein (2 μg/mL), or co-cultured with LAD2 cells (1×10^5) with or without RBD protein (B) for 48 h. In some groupss, Lor. (2.5 μg/mL), Eba. (1.5 μg/mL), or Ket. (4 μg/mL) was used to pretreat HULEC-5a cells for 2 h before stimulation (C). VE-cadherin was stained with specific antibodies and observed via fluorescence microscopy. Nucleus was stained with DAPI. Scale bar: 20 μm. D, E: VE-cadherin expression detected by flow cytometry. Cultured HULEC-5a cells were treated and immunostained as above, and VE-cadherin expression was detected by flow cytometry. Mean fluorescence intensity (MFI) was calculated. F, G: Spike/RBD-triggered MC activation for degranulation. LAD2 cells (3×10^5) were incubated with spike/RBD (2 μg/mL) at 37 °C for 1 h, fixed with 4% paraformaldehyde, permeabilized, immunostained with anti-avidin-FITC at 4 °C for 1 h, then analyzed by flow cytometry (F). Released histamines in cell culture supernatants were quantified by ELISA (G). Representative data are from four independent repeats.

co-culture with LAD2 cells in the presence of the spike/RBD protein (LAD2/RBD) (Figure 1E) decreased VE-cadherin expression. However, pretreatment of the HULEC-5a cells with the antihistamines rescued VE-cadherin impairment (Figure 1D, E).

We previously showed that SARS-CoV-2 spike/RBD triggers MCs to release cellular mediators (Wu et al, 2021). Here, the spike/RBD-induced rapid degranulation of MCs was confirmed by assessing the reduction in immunostaining intensity of cytoplasmic avidin particles (Figure 1F), and histamine released in the cell culture supernatants was quantified (Figure 1G).

Taken together, these results demonstrate that spike/RBD-triggered MC degranulation predisposes microvascular endothelial cells to damage.

Pretreatment of microvascular endothelial cells with antihistamines abolishes MC degranulation-induced inflammation

We next performed transcriptome analysis to examine inflammation in microvascular endothelial cells induced by MC

degranulation. The culture supernatants of spike/RBD-treated LAD2 cells were used to treat HULEC-5a cells for 24 h, after which the cell transcriptomes were analyzed using standard protocols. Data from five independent repeats were analyzed. As shown in the volcano plot, a total of 1 641 up-regulated genes and 835 down-regulated genes were identified in the HULEC-5a cells after treatment with the spike/RBD-treated LAD2 cell supernatant (Figure 2A). Gene Ontology (GO) functional enrichment analysis of differentially expressed genes (DEGs) showed obvious up-regulation of gene sets involved in cytokine signaling/production and inflammation regulation (Figure 2B). GSEA linked the up-regulated genes to inflammatory response regulation (Figure 2C). The core DEGs involved in the regulation of inflammation were catalogized, with significant enrichment in pro-inflammatory cytokine/chemokine-encoding genes, particularly S100 calcium binding protein A9 (*S100A9*), C-X-C motif chemokine ligand 11 *(CXCL11*), C-C motif chemokine ligand 7 (*CCL7*), C-X-C motif chemokine 10 (*CXCL10*), *IL-6*, and intercellular cell adhesion molecule-1 (*ICAM-1*) (Figure 2D). The expression levels of these significantly up-regulated cytokine/chemokine-encoding genes were confirmed using qRT-PCR (Figure 2E). Notably, pretreatment of the HULEC-5a cells with Ket., Eba., or Lor. significantly reduced MC degranulation-induced expression of these pro-inflammatory cytokines/chemokines (Figure 2E). IL-6 expression at the protein level was detected by intracellular immunostaining and flow cytometry, which confirmed the above findings (Figure 2F, G). Taken together, these results indicate that spike/RBD-triggered MC degranulation significantly induces inflammation in human microvascular endothelial cells, and pretreatment of cells with antihistamines abolishes the subsequent induction of inflammatory factors.

Combination of remdesivir and antihistamine reduces SARS-CoV-2 replication and inflammation and protects lung injury

We next investigated whether the co-administration of remdesivir and antihistamines can repress SARS-CoV-2 replication and alleviate inflammation. The 501Y.V2 strain of SARS-CoV-2 was used to infect wild-type BALB/c mice (Shuai et al, 2021). The spike/RBD of this variant triggered MC activation for rapid degranulation with dose-dependent effects (Supplementary Figure S1).

The BALB/c mice were treated with the antihistamine Lor. (10 mg/kg; i.p.) 1 day prior to intranasal infection with the 501Y.V2 variant (7.1×10^4 CCID50), then administered Lor. once daily until the mice were euthanized at 3 dpi. Remdesivir (25 mg/kg) was administered (i.p.) at the point of infection and used once daily until euthanasia (Figure 3A).

Compared with the infection group, the administration of Lor. and/or remdesivir did not further accelerate weight loss in mice (Figure 3B). As expected, the administration of remdesivir resulted in a 10-fold decrease in the SARS-CoV-2 viral load in the lung (Figure 3C). While administration of Lor. alone did not markedly suppress viral load (Figure 3C) (Wu et al, 2021), it significantly reduced the production of pro-inflammatory cytokines/chemokines, such as *IL-6*, tumor necrosis factor α (*TNF-α*), C-C motif chemokine ligand 5 (*CCL5*), *CXCL11*, C-C motif chemokine ligand 20 (*CCL20*), and *ICAM-1* (Figure 3D). Interestingly, while remdesivir showed incomplete inhibition of pro-inflammatory factor production, co-administration of Lor. and remdesivir greatly reduced pro-inflammatory factors to similar basal levels detected in the mock-infected controls (Figure 3D).

Frozen lung sections were immunostained for VE-cadherin to visualize pulmonary microvascular integrity (Wang et al, 2020a). SARS-CoV-2 infection disrupted the integrity, remdesivir alone maintained integrity to some extent, but completely preserved integrity when combined with Lor. (Figure 3E).

Mouse lung pathology was analyzed by H&E staining. Lung lesions, including alveolar septal thickening, inflammatory cell infiltration, mucosa desquamation, hyperemia, and hemorrhage, were observed in the SARS-CoV-2-infected mice (Figure 4A). Remdesivir administration reduced lung lesions, although damage still occurred. Notably, administration of Lor. or remdesivir/Lor. in combination greatly reduced lung lesions (Figure 4A). Pathological scores were assessed according to the degree of lung lesions in the tissue sections (Figure 4B). MCs and degranulation were indicated by metachromatic labeling with toluidine blue (Wu et al, 2021). SARS-CoV-2-induced peribronchial accumulation of MCs was observed and granule release was detected in the alveolar space (Figure 5B). Administration with remdesivir alone did not reduce MC accumulation or degranulation (Figure 5B). However, as observed previously (Wu et al, 2021), no MC accumulation or degranulation was observed in the Lor. or combined remdesivir/Lor. groups (Figure 5C–E).

Taken together, these results suggest that co-administration of remdesivir and antihistamines reduces viral replication and inhibits inflammation, thereby preventing lung damage.

DISCUSSION

Various therapeutic combinations have been trialed for the treatment of COVID-19, several of which have shown clinical improvement. For example, the addition of minocycline to favipiravir treatment significantly reduces pro-inflammatory cytokines IL-6 and IL-8 in COVID-19 patients (Itoh et al, 2022). The combination of the anti-inflammatory JAK1/2 inhibitor ruxolitinib and anti-C5a complement mAb eculizumab significantly decreases circulating D-dimer levels, reduces pulmonary lesions, and improves respiratory symptoms in severe COVID-19 patients (Giudice et al, 2020). Combined treatment of molnupiravir and favipiravir potentiates antiviral efficacy in SARS-CoV-2-infected hamsters (Abdelnabi et al, 2021). Triple antiviral therapy with interferon beta-1b, lopinavir-ritonavir, and ribavirin is superior to lopinavir/ritonavir alone in shortening viral shedding, alleviating disease symptoms, and facilitating recovery in patients with mild to moderate COVID-19 (Hung et al, 2020). In addition, two mAb combinations (casirivimab/imdevimab and bamlanivimab/etesevimab) have been authorized by the US FDA for emergency use to treat non-hospitalized COVID-19 patients with mild to moderate disease but at risk for clinical deterioration (Mouffak et al, 2021).

As the first antiviral drug formally approved for the treatment

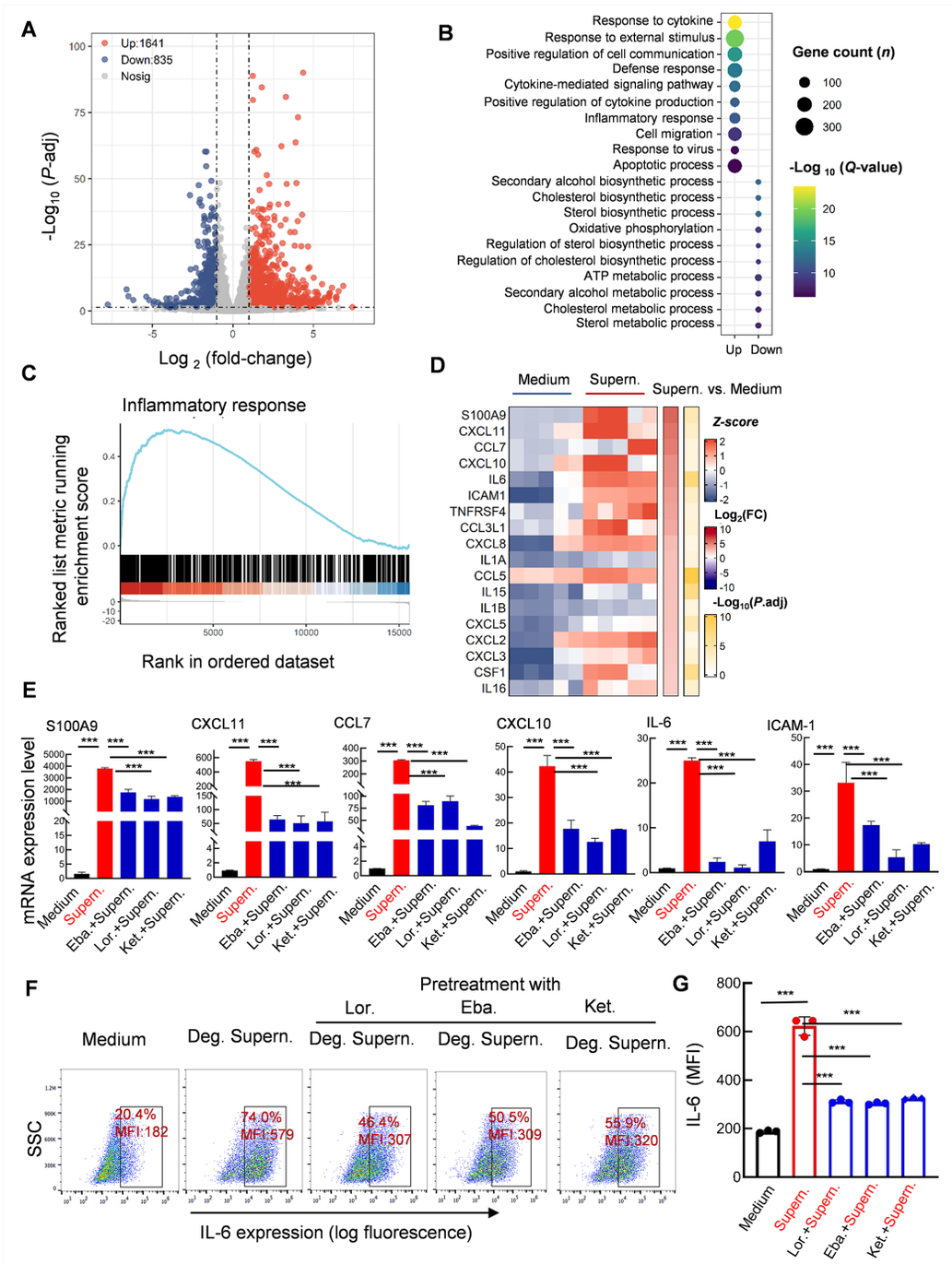

Figure 2 MC degranulation induces inflammation in human microvascular endothelial cells

HULEC-5a cells were stimulated with RBD-treated LAD2 cell culture supernatants for 24 h. Total RNA was extracted, and transcriptome analysis was performed. A: Volcano plot of DEGs comparing LAD2/RBD supernatant-treated versus medium-treated groups. Symbols of up-regulated and down-regulated genes are shown. B: GO functional enrichment analysis of DEGs. Color bar indicates minus logarithm of *q* values, and bubble size indicates absolute gene counts enriched in GO terms. C: GSEA of distribution of gene sets related to inflammatory response and enrichment scores based on DEGs. D: Heatmaps showing relative expression level (left panel), fold-change (middle panel), and adjusted *P*-values (right panel) for cytokine/chemokine-related genes. E: Pretreatment with antihistamines blocks expression of pro-inflammatory factors. HULEC-5a cells were pretreated with Lor. (2.5 μg/mL), Eba. (1.5 μg/mL), or Ket. (4 μg/mL) for 2 h before stimulation. Cellular mRNA levels of *S100A9*, *CXCL11*, *CCL7*, *CXCL10*, *IL-6*, and *ICAM-1* were quantified by qRT-PCR and normalized to *gapdh* mRNA. Representative data are from four independent repeats. F, G: IL-6 expression was detected by intracellular staining and flow cytometry. Three independent repeats are shown, MFI: Mean fluorescence intensity (G). Data are mean±standard deviation (*SD*). ***: *P*<0.001 indicates significant differences.

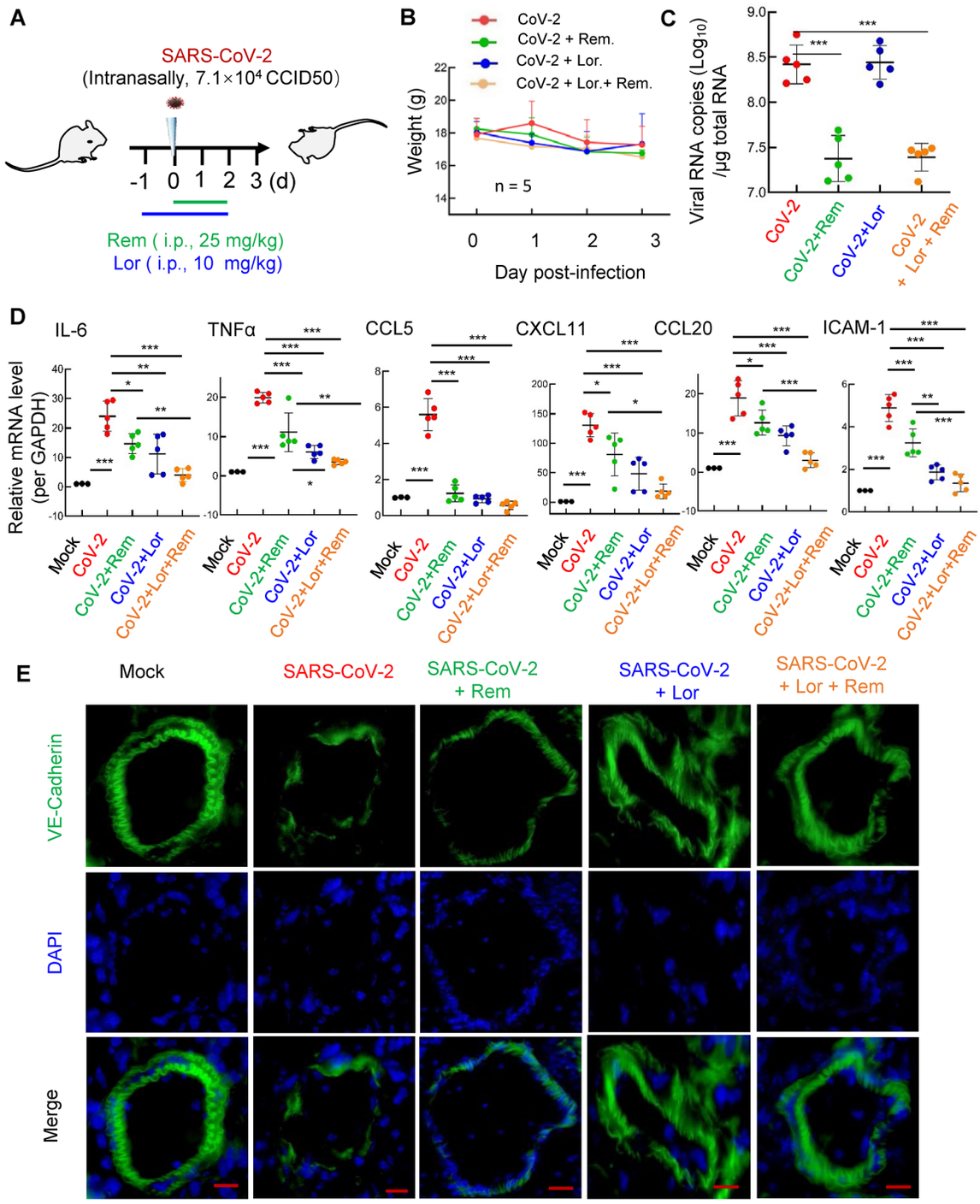

Figure 3 Combined remdesivir and Lor. treatment dampens SARS-CoV-2 replication and inflammation

A: Illustration of mouse treatments. BALB/c mice were infected intranasally with SARS-CoV-2 501Y.V2 strain (7.1×10^4 CCID50). In some mice, Lor. (10 mg/kg) was administered (i.p.) 1 day before infection, then given each day over the course of infection; remdesivir (25 mg/kg) was administered (i.p.) at the time of infection and used once daily until euthanasia. Each treatment group contained five mice; three mice without infection or drug treatment were used as mock controls. Lungs were collected at 3 dpi. B: Body weight was monitored. Mice were euthanized and lung lobes were harvested for analysis. C: Viral replication was monitored by quantifying expression of nucleocapsid gene. D: mRNA levels of *IL-6*, *TNF-α*, *CCL5*, *CXCL11*, *CCL20*, and *ICMA-1* were quantified using qRT-PCR and normalized to *gapdh* mRNA. E: Frozen lung sections were immunostained with VE-cadherin to indicate pulmonary microvascular integrity. Nucleus was stained with DAPI. Scale bar: 50 μm. Data are mean±*SD*. *: $P<0.05$; **: $P<0.01$; ***: $P<0.001$.

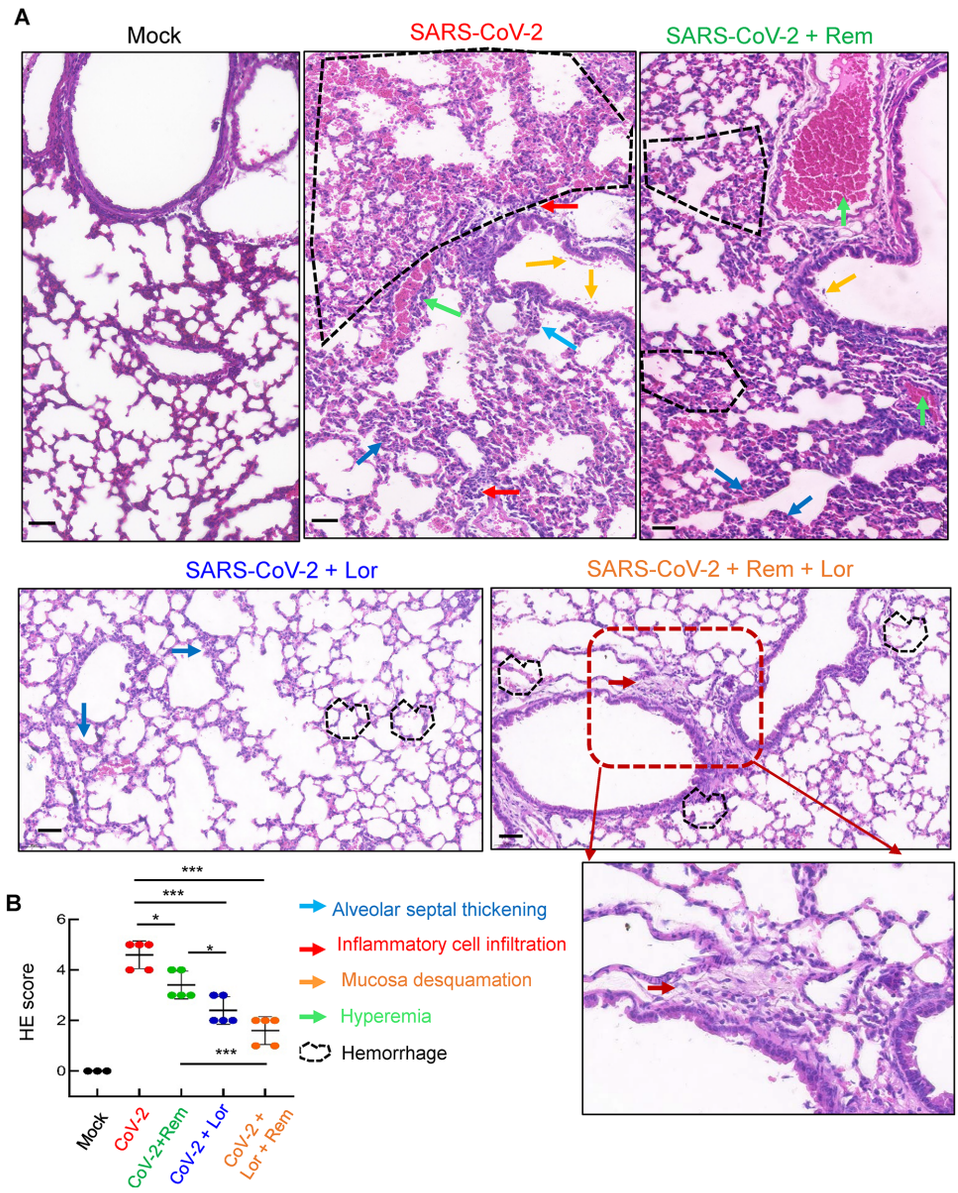

Figure 4 Combined remdesivir and Lor. treatment reduces lung lesions in SARS-CoV-2-infected mice

Lungs from above treated BALB/c mice were collected at 3 dpi. A: Pathological lung sections with H&E staining. Scale bar: 100 μm. B: H&E score in lung sections. Data are mean±*SD*. *: P<0.05; ***: P<0.001.

of COVID-19, remdesivir is a priority for developing drug combination. However, treatments used in combination with remdesivir are not limited to anti-inflammatory agents. For example, remdesivir with convalescent plasma shows clinical improvement in severe COVID-19 patients with X-linked agammaglobulinemia (Iaboni et al, 2021). Remdesivir shows synergistic effects at reducing viral replication in cell culture models when used in combination with the antifungal itraconazole (Schloer et al, 2021), antidepressant fluoxetine (Schloer et al, 2021), folate antagonist methotrexate (Stegmann et al, 2021), and Zn-ejector drugs disulfiram or ebselen (Chen et al, 2021). The combination of remdesivir and human soluble ACE2 also displays a strong additive effect on viral replication inhibition (Monteil et al, 2021).

When remdesivir is used in combination with anti-inflammatory agents, one crucial question is the timing for the administration of both components. Early administration of remdesivir shortens the time to clinical improvement in adult COVID-19 patients, but the benefit decreases or disappears when administered at the late phase of infection (Beigel et al, 2020; De Clercq, 2021; Rochwerg et al, 2020; Wang et al, 2020b), indicating that remdesivir should be administered as early as possible. Here, although remdesivir application at the time of infection significantly reduced pulmonary viral load and lung lesions in mice, it did not completely block the production of pro-inflammatory mediators and thus did not provide full protection against injury. It is possible that drug-inactivated viruses or viral components can still induce rapid inflammation

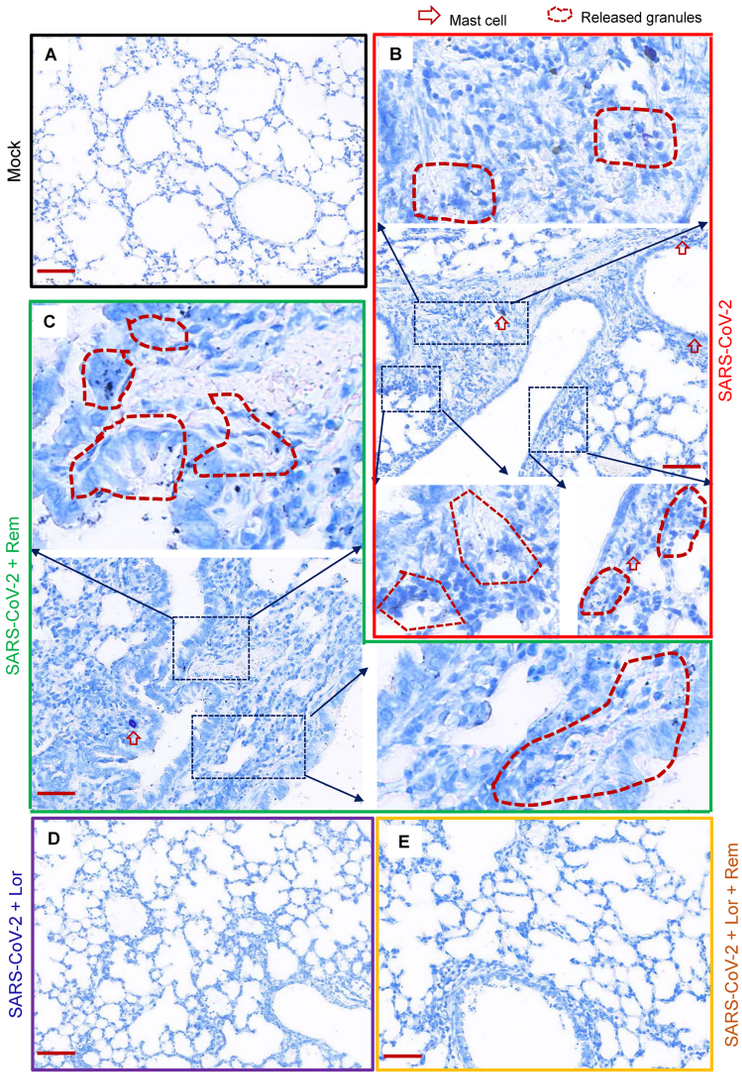

Figure 5 Administration of Lor. or Lor./remdesivir blocks MC accumulation

A: Mock infection. B: BALB/c mice were infected intranasally with SARS-CoV-2 501Y.V2 strain (7.1×10^4 CCID50). C: Remdesivir (25 mg/kg) was administered (i.p.) at time of infection and used once daily until euthanasia. D, E: In some mice, Lor. (10 mg/kg) was administered (i.p.) 1 day before infection, then continued each day over the course of infection. Lungs were collected at 3 dpi. Toluidine blue staining of lung sections was used to observe MCs and their degranulation. Scale bar: 100 μm.

and sequential immune cascades, causing tissue injury (Rauti et al, 2021). Thus, anti-inflammatory agents should also be applied as early as possible before the onset of the inflammatory response. Inadequate blockade of inflammation may account for the lack of clinical benefit found when tocilizumab or corticosteroids are combined with remdesivir (Garibaldi et al, 2021; Rosas et al, 2021). In our study, early combined treatment with the antihistamine loratadine and remdesivir showed complete repression of pro-inflammatory mediator production in infected mice, highlighting the need for early administration of anti-inflammatory agents.

Growing evidence suggests that MCs play critical roles in the pathogenesis of SARS-CoV-2 (Lam et al, 2021; Malone et al, 2021; Murdaca et al, 2021). We recently found that SARS-CoV-2-induced MC degranulation initiates alveolar epithelial inflammation and causes lung lesions in ACE2-humanized mice (Wu et al, 2021). MCs have also been proposed as novel therapeutic cellular targets for the treatment of COVID-19 (Lam et al, 2021; Malone et al, 2021; Murdaca et al, 2021). Repurposed famotidine, a histamine-2 receptor (HR2) antagonist, significantly improves pulmonary symptoms in COVID-19 patients (Freedberg et al, 2020; Janowitz et al, 2020; Malone et al, 2021). Famotidine has also been shown to inhibit Toll-like receptor 3-mediated inflammatory signaling in SARS-CoV-2 infection (Mukherjee et al, 2021). Administration of famotidine in combination with the HR1 antagonist cetirizine has also been shown to reduce mortality in COVID-19 patients (Hogan Ii et al, 2020; Mather et al, 2020). We previously demonstrated that the antihistamines ebastine and loratadine, as MC stabilizers blocking degranulation, can dampen SARS-CoV-2-induced production of pro-inflammatory factors, thereby preventing lung injury in mice (Wu et al, 2021). In this study,

these HR1 antagonists were used to pre-block microvascular endothelial cells, resulting in significant repression of inflammatory mediator production in target cells. Importantly, co-administration of loratadine with remdesivir dampened both SARS-CoV-2 replication and inflammation and protected mice from lung injury.

Taken together, our results emphasize the critical role of MCs in the pathogenesis of SARS-CoV-2 and demonstrate the versatile benefit of antihistamine and remdesivir co-administration in suppressing viral replication and alleviating inflammation in a mouse model of SARS-CoV-2 infection. Our findings provide a feasible approach to combine antiviral and anti-inflammatory agents for COVID-19 treatment. Thus, the clinical benefits warrant further investigation.

DATA AVAILABILITY

All raw RNA-seq data used in this study have been deposited at the National Genomics Data Center (BioProjectID PRJCA007111, https://bigd.big.ac.cn/gsa-human/browse/HRA001517), Science Data Bank (Data doi:10.11922/sciencedb.01655, https://www.scidb.cn/s/MBb6r2), and NCBI (BioProjectID PRJNA822440, http://www.ncbi.nlm.nih.gov/bioproject/822440).

SUPPLEMENTARY DATA

Supplementary data to this article can be found online.

COMPETING INTERESTS

The authors declare that they have no competing interests.

AUTHORS' CONTRIBUTIONS

Conceptualization: J.H.W.; Data Curation and Visualization: M.L.W., F.L.L., J.S., and X.L. Formal Analysis: M.L.W. and J.H.W.; Resources: J.H.W., J.C.Z., J.S., J.R.Q., X.J., Y.T.Z., and X.W.C.; Software: Q.H.Y.; Writing-Original Draft: M.L.W. and J.H.W.; Writing-Review & Editing: X.J. and J.H.W.; Project Administration: J.H.W., J.C.Z., and Y.T.Z.; Supervision: J.H.W. All authors read and approved the final version of the manuscript.

ACKNOWLEDGEMENTS

We thank Prof. Ling Chen for reagents.

REFERENCES

Abdelaziz MM, Khair OA, Devalia JL. 2000. The potential of active metabolites of antihistamines in the management of allergic disease. *Allergy*, **55**(5): 425−434.

Abdelnabi R, Foo CS, Kaptein SJF, Zhang X, Do TND, Langendries L, et al. 2021. The combined treatment of Molnupiravir and Favipiravir results in a potentiation of antiviral efficacy in a SARS-CoV-2 hamster infection model. *eBioMedicine*, **72**: 103595.

Attiq A, Yao LJ, Afzal S, Khan MA. 2021. The triumvirate of NF-κB, inflammation and cytokine storm in COVID-19. *International Immunopharmacology*, **101**: 108255.

Beigel JH, Tomashek KM, Dodd LE, Mehta AK, Zingman BS, Kalil AC, et al. 2020. Remdesivir for the treatment of covid-19 - final report. *The New England Journal of Medicine*, **383**(19): 1813−1826.

Benfield T, Bodilsen J, Brieghel C, Harboe ZB, Helleberg M, Holm C, et al. 2021. Improved survival among hospitalized patients with coronavirus disease 2019 (COVID-19) treated with remdesivir and dexamethasone. A nationwide population-based cohort study. *Clinical Infectious Diseases*, **73**(11): 2031−2036.

Biswas P, Hasan MM, Dey D, Dos Santos Costa AC, Polash SA, Bibi S, et al. 2021. Candidate antiviral drugs for COVID-19 and their environmental implications: a comprehensive analysis. *Environmental Science and Pollution Research*, **28**(42): 59570−59593.

Chen NS, Zhou M, Dong X, Qu JM, Gong FY, Han Y, et al. 2020. Epidemiological and clinical characteristics of 99 cases of 2019 novel coronavirus pneumonia in Wuhan, China: a descriptive study. *The Lancet*, **395**(10223): 507−513.

Chen T, Fei CY, Chen YP, Sargsyan K, Chang CP, Yuan HS, et al. 2021. Synergistic inhibition of SARS-CoV-2 replication using disulfiram/ebselen and remdesivir. *ACS Pharmacology & Translational Science*, **4**(2): 898−907.

Da Silva Motta Junior J, Dos Santos Miggiolaro AFR, Nagashima S, De Paula CBV, Baena CP, Scharfstein J, et al. 2020. Mast cells in alveolar septa of COVID-19 patients: a pathogenic pathway that may link interstitial edema to immunothrombosis. *Frontiers in Immunology*, **11**: 574862.

Daher J. 2021. Endothelial dysfunction and COVID-19 (Review). *Biomedical Reports*, **15**(6): 102.

De Clercq E. 2021. Remdesivir: Quo vadis?. *Biochemical Pharmacology*, **193**: 114800.

Dos Santos Miggiolaro AFR, Da Silva Motta Junior J, De Paula CBV, Nagashima S, Malaquias MAS, Carstens LB, et al. 2020. Covid-19 cytokine storm in pulmonary tissue: Anatomopathological and immunohistochemical findings. *Respiratory Medicine Case Reports*, **31**: 101292.

Freedberg DE, Conigliaro J, Wang TC, Tracey KJ, Callahan MV, Abrams JA, et al. 2020. Famotidine use is associated with improved clinical outcomes in hospitalized COVID-19 patients: a propensity score matched retrospective cohort study. *Gastroenterology*, **159**(3): 1129−1131.E3.

Garibaldi BT, Wang KB, Robinson ML, Zeger SL, Bandeen-Roche K, Wang MC, et al. 2021. Comparison of time to clinical improvement with vs without remdesivir treatment in hospitalized patients with COVID-19. *JAMA Network Open*, **4**(3): e213071.

Giudice V, Pagliano P, Vatrella A, Masullo A, Poto S, Polverino BM, et al. 2020. Combination of ruxolitinib and eculizumab for treatment of severe SARS-CoV-2-related acute respiratory distress syndrome: a controlled study. *Frontiers in Pharmacology*, **11**: 857.

Hogan II RB, Hogan III RB, Cannon T, Rappai M, Studdard J, Paul D, et al. 2020. Dual-histamine receptor blockade with cetirizine - famotidine reduces pulmonary symptoms in COVID-19 patients. *Pulmonary Pharmacology & Therapeutics*, **63**: 101942.

Huang CL, Huang LX, Wang YM, Li X, Ren LL, Gu XY, et al. 2021. 6-month consequences of COVID-19 in patients discharged from hospital: a cohort study. *The Lancet*, **397**(10270): 220−232.

Hung IFN, Lung KC, Tso EYK, Liu R, Chung TWH, Chu MY, et al. 2020. Triple combination of interferon beta-1b, lopinavir-ritonavir, and ribavirin in the treatment of patients admitted to hospital with COVID-19: an open-label, randomised, phase 2 trial. *The Lancet*, **395**(10238): 1695−1704.

Iaboni A, Wong N, Betschel SD. 2021. A patient with X-linked agammaglobulinemia and COVID-19 infection treated with remdesivir and convalescent plasma. *Journal of Clinical Immunology*, **41**(5): 923−925.

Itoh K, Sakamaki I, Hirota T, Iwasaki H. 2022. Evaluation of minocycline combined with favipiravir therapy in coronavirus disease 2019 patients: a case-series study. *Journal of Infection and Chemotherapy*, **28**(1): 124−127.

Janowitz T, Gablenz E, Pattinson D, Wang TC, Conigliaro J, Tracey K, et al. 2020. Famotidine use and quantitative symptom tracking for COVID-19 in non-hospitalised patients: a case series. *Gut*, **69**(9): 1592−1597.

Kalil AC, Patterson TF, Mehta AK, Tomashek KM, Wolfe CR, Ghazaryan V, et al. 2021. Baricitinib plus remdesivir for hospitalized adults with covid-19. *The New England Journal of Medicine*, **384**(9): 795−807.

Komi DEA, Wöhrl S, Bielory L. 2020. Mast cell biology at molecular level: a comprehensive review. *Clinical Reviews in Allergy & Immunology*, **58**(3): 342−365.

Konkolova E, Dejmek M, Hřebabecký H, Šála M, Böserle J, Nencka R, et al. 2020. Remdesivir triphosphate can efficiently inhibit the RNA-dependent RNA polymerase from various flaviviruses. *Antiviral Research*, **182**: 104899.

Lam HY, Tergaonkar V, Kumar AP, Ahn KS. 2021. Mast cells: therapeutic targets for COVID-19 and beyond. *IUBMB Life*, **73**(11): 1278−1292.

Mahase E. 2021a. Covid-19: molnupiravir reduces risk of hospital admission or death by 50% in patients at risk, MSD reports. *BMJ*, **375**: n2422.

Mahase E. 2021b. Covid-19: Pfizer's paxlovid is 89% effective in patients at risk of serious illness, company reports. *BMJ*, **375**: n2713.

Mahase E. 2021c. Covid-19: UK becomes first country to authorise antiviral molnupiravir. *BMJ*, **375**: n2697.

Malone RW, Tisdall P, Fremont-Smith P, Liu YF, Huang XP, White KM, et al. 2021. COVID-19: famotidine, histamine, mast cells, and mechanisms. *Frontiers in Pharmacology*, **12**: 633680.

Marfe G, Perna S, Shukla AK. 2021. Effectiveness of COVID-19 vaccines and their challenges (Review). *Experimental and Therapeutic Medicine*, **22**(6): 1407.

Mather JF, Seip RL, McKay RG. 2020. Impact of famotidine use on clinical outcomes of hospitalized patients with COVID-19. *The American Journal of Gastroenterology*, **115**(10): 1617−1623.

Monteil V, Dyczynski M, Lauschke VM, Kwon H, Wirnsberger G, Youhanna S, et al. 2021. Human soluble ACE2 improves the effect of remdesivir in SARS-CoV-2 infection. *EMBO Molecular Medicine*, **13**(1): e13426.

Mouffak S, Shubbar Q, Saleh E, El-Awady R. 2021. Recent advances in management of COVID-19: a review. *Biomedicine & Pharmacotherapy*, **143**: 112107.

Mukherjee R, Bhattacharya A, Bojkova D, Mehdipour AR, Shin D, Khan KS, et al. 2021. Famotidine inhibits toll-like receptor 3-mediated inflammatory signaling in SARS-CoV-2 infection. *Journal of Biological Chemistry*, **297**(2): 100925.

Murdaca G, Di Gioacchino M, Greco M, Borro M, Paladin F, Petrarca C, et al. 2021. Basophils and mast cells in COVID-19 pathogenesis. *Cells*, **10**(10): 2754.

Pruijssers AJ, George AS, Schäfer A, Leist SR, Gralinksi LE, Dinnon KH III, et al. 2020. Remdesivir inhibits SARS-CoV-2 in human lung cells and chimeric SARS-CoV expressing the SARS-CoV-2 RNA polymerase in mice. *Cell Reports*, **32**(3): 107940.

Qin C, Zhou LQ, Hu ZW, Zhang SQ, Yang S, Tao Y, et al. 2020. Dysregulation of immune response in patients with coronavirus 2019 (COVID-19) in Wuhan, China. *Clinical Infectious Diseases*, **71**(15): 762−768.

Rauti R, Shahoha M, Leichtmann-Bardoogo Y, Nasser R, Paz E, Tamir R, et al. 2021. Effect of SARS-CoV-2 proteins on vascular permeability. *eLife*, **10**: e69314.

Rochwerg B, Agarwal A, Zeng LN, Leo YS, Appiah JA, Agoritsas T, et al. 2020. Remdesivir for severe covid-19: a clinical practice guideline. *BMJ*, **370**: m2924.

Rosas IO, Diaz G, Gottlieb RL, Lobo SM, Robinson P, Hunter BD, et al. 2021. Tocilizumab and remdesivir in hospitalized patients with severe COVID-19 pneumonia: a randomized clinical trial. *Intensive Care Medicine*, **47**(11): 1258−1270.

Rubin D, Chan-Tack K, Farley J, Sherwat A. 2020. FDA approval of remdesivir - a step in the right direction. *New England Journal of Medicine*, **383**(27): 2598−2600.

Schloer S, Brunotte L, Mecate-Zambrano A, Zheng SY, Tang J, Ludwig S, et al. 2021. Drug synergy of combinatory treatment with remdesivir and the repurposed drugs fluoxetine and itraconazole effectively impairs SARS-CoV-2 infection in vitro. *British Journal of Clinical Pharmacology*, **178**(11): 2339−2350.

Shuai HP, Chan JFW, Yuen TTT, Yoon C, Hu JC, Wen L, et al. 2021. Emerging SARS-CoV-2 variants expand species tropism to murines. *eBioMedicine*, **73**: 103643.

Slater JW, Zechnich AD, Haxby DG. 1999. Second-generation antihistamines: a comparative review. *Drugs*, **57**(1): 31−47.

Song TZ, Zheng HY, Han JB, Jin L, Yang X, Liu FL, et al. 2020. Delayed severe cytokine storm and immune cell infiltration in SARS-CoV-2-infected aged Chinese rhesus macaques. *Zoological Research*, **41**(5): 503−516.

Stegmann KM, Dickmanns A, Gerber S, Nikolova V, Klemke L, Manzini V, et al. 2021. The folate antagonist methotrexate diminishes replication of the coronavirus SARS-CoV-2 and enhances the antiviral efficacy of remdesivir in cell culture models. *Virus Research*, **302**: 198469.

Tian RR, Yang CX, Zhang M, Feng XL, Luo RH, Duan ZL, et al. 2021. Lower respiratory tract samples are reliable for severe acute respiratory syndrome coronavirus 2 nucleic acid diagnosis and animal model study. *Zoological Research*, **42**(2): 161−169.

Wang DW, Hu B, Hu C, Zhu FF, Liu X, Zhang J, et al. 2020a. Clinical characteristics of 138 hospitalized patients with 2019 novel coronavirus-infected pneumonia in Wuhan, China. *JAMA*, **323**(11): 1061−1069.

Wang P, Luo RH, Zhang M, Wang YQ, Song TZ, Tao TT, et al. 2020b. A cross-talk between epithelium and endothelium mediates human alveolar-capillary injury during SARS-CoV-2 infection. *Cell Death & Disease*, **11**(12): 1042.

Wang YM, Zhang DY, Du GH, Du RH, Zhao JP, Jin Y, et al. 2020c. Remdesivir in adults with severe COVID-19: a randomised, double-blind, placebo-controlled, multicentre trial. *The Lancet*, **395**(10236): 1569−1578.

Wu ML, Liu FL, Sun J, Li X, He XY, Zheng HY, et al. 2021. SARS-CoV-2-triggered mast cell rapid degranulation induces alveolar epithelial inflammation and lung injury. *Signal Transduction and Targeted Therapy*, **6**(1): 428.

Xu L, Yu DD, Ma YH, Yao YL, Luo RH, Feng XL, et al. 2020. COVID-19-like symptoms observed in Chinese tree shrews infected with SARS-CoV-2. *Zoological Research*, **41**(5): 517−526.

Ye ZW, Yuan SF, Chan JFW, Zhang AJ, Yu CY, Ong CP, et al. 2021. Beneficial effect of combinational methylprednisolone and remdesivir in hamster model of SARS-CoV-2 infection. *Emerging Microbes & Infections*, **10**(1): 291−304.

Zhou YY, Zhou B, Pache L, Chang M, Khodabakhshi AH, Tanaseichuk O, et al. 2019. Metascape provides a biologist-oriented resource for the analysis of systems-level datasets. *Nature Communications*, **10**(1): 1523.